Numerical formulation for advanced analysis of semi-rigid steel-concrete composite frames

Luiz O. M. Teles[1], Ígor J.M. Lemes[2], Ricardo A.M. Silveira[1], Rafael C. Barros[3]

[1]*Department of Civil Engineering , Federal University of Ouro Preto*
Ouro Preto, 35400-000, Minas Gerais, Brazil
luiz.teles@ufop.edu.br, ricardo@ufop.edu.br
[2]*Department of Engineering, Federal University of Lavras*
Lavras, 37200-000, Minas Gerais, Brazil
igor.lemes@ufla.br
[3]*Sereng Engineering and Consulting*
rafaelcesario@hotmail.com

Abstract. The present work aims at the implementation and validation of a displacement-based two-dimensional numerical formulation including several sources of non-linearities in steel-concrete composite frames, such as second-order effects, plasticity and beam-to-column semi-rigid connections. The co-rotational based approach is used to describe the finite element formulation, allowing large displacements and rotations in the numerical model. Two rotational pseudo-springs in series are positioned at the finite element ends. One of them is used to include the gradual loss of stiffness determined by the cross-sectional plastification, where the axial and flexural stiffnesses are homogenized for improve accuracy in capturing the interaction between bending moments and axial forces. The limiting of the uncracked, elastic, and plastic regimes is defined in the axial force-bending moment diagram. In the cross-sectional analysis, the Strain Compatibility Method (SCM) and the Refined Plastic Hinge Method (RPHM) are used to capture the axial strains in the section components. In this way, the uniaxial constitutive models of the materials are described by continuous functions. The cracked effect is considered by the effective moment of inertia of the concrete cross-section. The other spring includes the effects of the semi-rigid beam-to-column connections through the moment-rotation relationship. A three-parameter power model for beam-to-column connections is used. To validate the proposed numerical formulation, the results obtained are compared with numerical and experimental data available in the literature. These comparisons indicated validation of the numerical procedure proposed and implemented here, highlighting the precision of the formulation in both pre- and post-critical structural behavior.

Keywords: Numerical formulation, Advanced Analysis, Steel-concrete composite frames, Co-rotational approach and Finite element method

1 Introduction

There are three basic pillars for the development of a structural project: safety, time (both in design and execution), and cost-efficiency. The optimization of these three variables is primarily related to the materials and methods of analysis used. In civil construction, when it comes to material selection, Lemes [1] and Caldas [2] highlighted that steel and concrete are the most common, as their combination allows for better physical and mechanical utilization of their properties.

The main advantages of steel-concrete composite structures are increased strength and rigidity, protection of steel elements (from fire and corrosion), and cost benefits. Lemes [1] added that this type of structural system also has execution advantages, as steel profiles can support concrete elements during the concrete curing process. This condition reduces costs associated with formwork and increases free space for material circulation on the construction site.

However, Lemes [1] warned that this type of structural system presents various forms of instability. In the pursuit of optimizing its behavior, advanced computational analysis stands out, as it allows for the development of numerical processes that can solve problems that would be unfeasible with traditional analytical methods and simplified design standards. The combination of steel and concrete has also become a viable solution for the

rehabilitation of old structures, as evidenced by de Oliveira [3], offering an economical and sustainable alternative.

In this context, a crucial element to be investigated is the connections between beams and columns, especially considering their semi-rigid conditions. Lemes [1] explained that, in numerical analysis, semi-rigid beam-to-column connections are typically represented using spring elements at the joints. Lemes [1] cited this approach for capturing the flexural behavior of the connection. Weng and Yen [4] demonstrated that composite structures can closely or distantly resemble real structural behavior depending on different analysis forms in various design standards. The ongoing search for more accurate formulations and faster solution methodologies remains essential in structural engineering practice.

2 Methodology

In this study, a formulation based on the Refined Plastic Hinge Method (RPHM) with a co-rotational approach was applied. This methodology assesses all previously discussed effects. It uses a hybrid finite element of length L. Two series pseudo-springs with zero length are used at each end of the element. The outer springs are associated with the flexibility of the connection with rotational stiffness S_c, where the moment-rotation relationship describes the beam-to-column joint behavior. The inner springs are linked to the material's inelastic behavior, represented by S_s, which considers the effects from the onset of yielding to full yield. Notably, although the element is used throughout the discretization, only at the nodes where the beam and column are connected are the effects on the S_c parameter considered.

Referencing this element to the local system through the co-rotational approach, the actual displacements are the rotations at nodes i and j (θ_{ci}, θ_{cj}) and the axial displacement δ. The corresponding forces are M_{ci}, M_{cj}, and N. The deformed configuration of the hybrid element is shown in Figure 1.

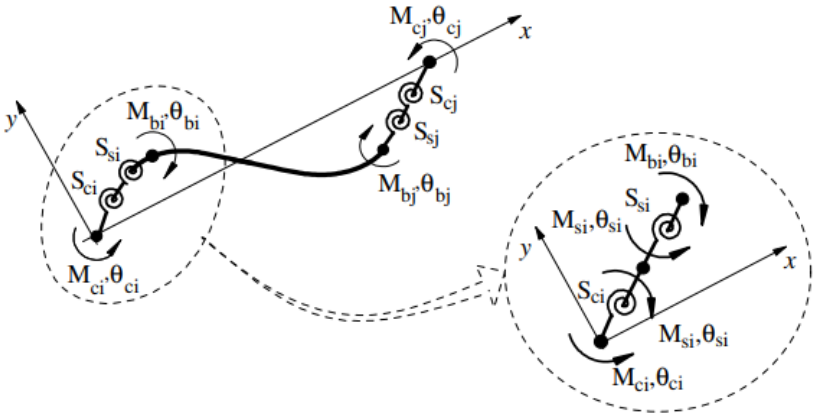

Figure 1. Deformed hybrid finite element [5]

Chen et al. [6] noted that for most steel structures, axial and shear forces have minimal effects on joint deformation compared to bending moments. In a two-dimensional analysis, torsion is also neglected, meaning semi-rigid joints are simulated considering only flexural rotation.

Starting from the deformed finite element, each pseudo-spring is governed by kinematic, equilibrium, and uniaxial constitutive relations, respectively $\phi_c = \theta_c - \theta_b$, $M_c + M_b = 0$ and $M_c = S_c\phi_c$. Where ϕ_c is the relative rotation of the spring given by the difference between the connection angle θ_c and the beam-to-column rotation θ_b [7]; S_c is the connection stiffness derived from the $M \times \phi$ relationship; M_c and M_b are the moments in the spring and beam-to-column elements, respectively.

The combining with the beam-to-column element parameters, and noting that the incremental internal moments ΔM_{si} and ΔM_{sj} are zero (as loads are applied at global external nodes), the following moment-rotation relationship is obtained:

$$\begin{Bmatrix} \Delta M_{ci} \\ \Delta M_{bi} \\ \Delta M_{bj} \\ \Delta M_{cj} \end{Bmatrix} = \begin{bmatrix} S_{sci} & -S_{sci} & 0 & 0 \\ -S_{sci} & k_{(2,2)} + S_{sci} & k_{(3,2)} & 0 \\ 0 & k_{(2,3)} & k_{(3,3)} + S_{scj} & -S_{scj} \\ 0 & 0 & -S_{scj} & S_{scj} \end{bmatrix} \begin{Bmatrix} \Delta\theta_{ci} \\ \Delta\theta_{bi} \\ \Delta\theta_{bj} \\ \Delta\theta_{cj} \end{Bmatrix} \tag{1}$$

where S_{csi} and S_{csj} are parameters evaluating the combined effects of semi-rigidity and steel inelasticity at the nodal points i and j of the hybrid element, respectively. These parameters represent the equivalent stiffness of the spring elements and are defined as [5]:

$$S_{sci} = \frac{S_{ci}S_{si}}{S_{ci} + S_{si}} \quad and \quad S_{scj} = \frac{S_{cj}S_{sj}}{S_{cj} + S_{sj}} \tag{2}$$

Thus, S_c can be determined using one of the mathematical models representing the moment-rotation behavior as demonstrated in Section 2.1, and the cross-section resistance parameter S_s can be calculated according to Fong and Chan [8] by the following equation:

$$S_s = \frac{E_a I_{hom}}{L}\left(\frac{M_{pr} - M}{M - M_{er}}\right) \tag{3}$$

where L is the length of the finite element, E_a is the steel's modulus of elasticity, and I_{hom} represents the homogenized moment of inertia of the composite section evaluated at nodes i and j. The process of section homogenization to obtain I_{hom} is discussed and demonstrated by Lemes [1] and presented later in this paper.

Silva [5] and Lemes [1] explain that for an elastic section, the spring stiffness is infinite, allowing full moment transfer from one side of the spring element to the other, with S_s numerically defined as $S_s = 10^{10}$. When the moment is below the yield moment M_{er}, the section remains elastic with virtually infinite spring stiffness. As the acting moment reaches the yield moment, there is a progressive reduction in section stiffness. With section yield, S_s reduces to zero, numerically defined as $S_s = 10^{-10}$, effectively nullifying the spring stiffness and simulating the formation of a plastic hinge when the moment reaches the plastic moment M_{pr}, indicating the nullification of spring stiffness and absence of moment transfer.

The presented formulation considers material nonlinearity exclusively at the finite element nodes, meaning the element remains linearly elastic along its length. According to Lemes [1], for situations where the material in a prismatic element behaves elastically, the system's strain energy (U) can be written as:

$$U = \frac{EA}{2}\int_0^L \varepsilon^2 dx + \frac{EI}{2}\int_0^L \Phi^2 dx \tag{4}$$

where L is the element length, EA and EI are the axial and flexural stiffnesses of the cross-section, and ε (axial) and Φ (curvature) are the associated strains. Based on Euler-Bernoulli theory, the degenerate form of Green's strain and curvature can be expressed as [9]:

$$\varepsilon = \frac{du}{dx} + \frac{1}{2}\left(\frac{dv}{dx}\right)^2 \quad \text{and} \quad \Phi = -\frac{d^2v}{dx^2} \tag{5}$$

where u and v are the axial and vertical displacements of the element. Interpolation functions are applied to describe these displacements, with cubic Hermite polynomials used for vertical displacements and the equation defined by Tang et al. [10] for axial displacements. Thus:

$$v = x\left(1 - \frac{x}{L}\right)^2 \theta_i + \frac{x^2}{L}\left(\frac{x}{L} - 1\right)\theta_j \tag{6}$$

$$u = \frac{x}{L}\delta + \frac{x}{L}\int_0^L \frac{1}{2}\left(\frac{dv}{dx}\right)^2 dx - \int_0^x \frac{1}{2}\left(\frac{dv}{dx}\right)^2 dx \tag{7}$$

Stiffness matrix terms are defined by the second variation of strain energy or the first derivative of the internal force vector as follows:

$$\mathbf{K}_l = \frac{\partial^2 U}{\partial \mathbf{u}_l^2} = \frac{\partial \mathbf{f}_l}{\partial \mathbf{u}_l} \tag{8}$$

Appropriately refined meshes are used to account for yield effects exclusively at the finite element nodes (plastic hinge approach) [1], implying only nodal loads simulate external forces, leading to a linear variation of bending moments along the elements' length [11]. The moment of inertia, considering cracking, is determined by the following equation [1]:

$$I_{hom}(x) = \left(1 - \frac{x}{L}\right) I_{hom,i} + \frac{x}{L} I_{hom,j} \tag{9}$$

where L is the element length and I_{hom} is the homogenized moment of inertia of the composite section evaluated at nodes i and j, as defined by:

$$I_{hom} = I_a + \frac{E_r}{E_a} I_r + \frac{E_c}{E_a} I_{ef} \tag{10}$$

where I_a is the moment of inertia of the steel, E_r is the modulus of elasticity of the reinforcement, and E_c is the modulus of elasticity of the concrete, as calculated according to Lemes [1]. The term I_r represents the moment of inertia of the reinforcement, while I_{ef} denotes the effective moment of inertia of the concrete section, which accounts for the cracked region of the concrete.

Using the second derivatives of the functions (terms of the vector **N** [1]) consistent with the cubic Hermite polynomials in Equation 6, the bending stiffness matrix terms are determined by:

$$\mathbf{k}_l^* = \int_0^L \mathbf{N}^T I_{hom}(x)\, \mathbf{N} dx \tag{11}$$

Considering all degrees of freedom, the beam-to-column element stiffness matrix is calculated as follows:

$$k_{l,22} = \frac{E_a (3I_{hom,i} + I_{hom,j})}{L} + \frac{2NL}{15} \tag{12}$$

$$k_{l,23} = k_{l,32} = \frac{E_a (I_{hom,i} + I_{hom,j})}{L} - \frac{NL}{30} \tag{13}$$

$$k_{l,33} = \frac{E_a (I_{hom,i} + 3I_{hom,j})}{L} + \frac{2NL}{15} \tag{14}$$

where N is the internal axial force and E_a is the steel's elasticity modulus. Axial stiffnesses are determined by averaging the nodal responses [1], and terms of this matrix are referenced as $k_{le,mn}$, where le denotes the beam column element and m and n indicate the positions of the terms (row and column of $\mathbf{k}_{le}$, respectively).

The parameter $(k_{l,11})$ considers the axial degree of freedom of the element via the homogenized cross-section (A_{hom}) and is expressed as:

$$k_{l,11} = \frac{E_a A_{hom}}{L} \tag{15}$$

The additional terms $k_{le,22}$, $k_{le,23}$, $k_{le,32}$, and $k_{le,33}$ carry more weight than the higher-order terms derived by Yang and Kuo [12]. Previous studies [1, 13] indicate that the precision of numerical simplification does not affect the system's overall response, even in highly nonlinear problems.

2.1 Three-Parameter Power Model

Beam-to-column connections are crucial for structural integrity, as they transfer loads and impact the system's capacity. Accurate performance is vital for resisting gravitational and lateral forces. Several authors have proposed models to simulate these connections, including the three-parameter power model (3PP) by [14]. This model is valued for its simplicity, requiring only three parameters: initial stiffness ($S_{c,ini}$), final moment capacity (M_u), and a shape parameter (n). The moment-rotation relationship is given by:

$$M = \frac{S_{c,ini}\phi_c}{\left[1 + \left(\frac{S_{c,ini}\phi_c}{M_u}\right)^n\right]^{1/n}} \tag{16}$$

where $S_{c,ini}$ is the initial stiffness, M_u is the final bending moment capacity, and n defines the curve's shape.

3 Numerical Results

The present section analyzes two semi-rigid one-story frames, as proposed and simulated by Bui and Kim [15] and Bui et al. [14] using their own formulations and the software ABAQUS [16]. One frame has columns with a circular cross-section [15], while the other has columns with a rectangular cross-section [14]. Both structures are composed of HEA200 steel I-section beams, with columns filled with concrete in steel tubes. As illustrated in Figure 2(a), two incremental vertical loads P = 2800 kN are applied to the top ends of the columns, and an incremental lateral load (H = 35 kN) is applied to the top of the left column. The figure also shows the dimensions, which are identical for both frames, with an effective span length of 3.0 m and an effective column height of 2.905 m.

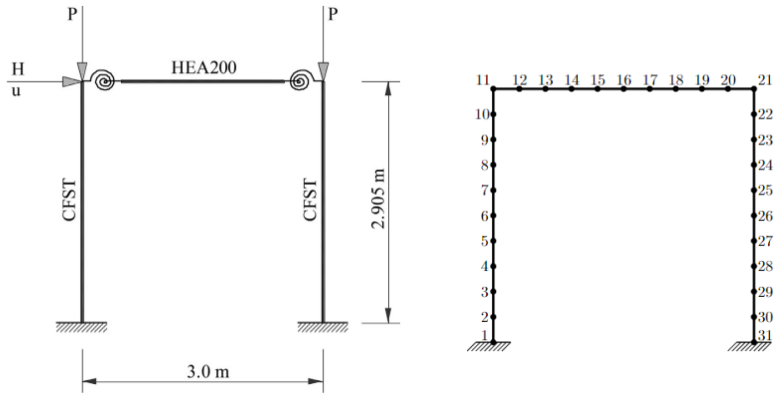

(a) Dimensions (b) Finite element discretization

Figure 2. Simple frames with composite columns and steel beam

Figure 3 shows the detailed cross-sections of the circular and retangular columns filled with concrete. In both structures, the steel tubes have the following properties: modulus of elasticity (E_s) = 200 GPa, yield strength (f_y) of 250 MPa, and ultimate strength (f_u) of 400 MPa. Additionally, the compressive strength (f_c) of the concrete cores was considered to be 38 MPa.

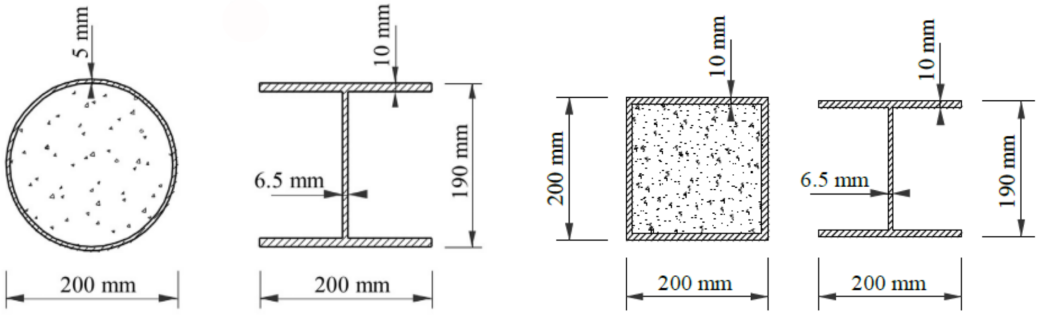

(a) Columns with circular section (b) Columns with rectangular section

Figure 3. Cross-sections [14, 15]

The authors make it clear that the structure was subjected to simulations with semi-rigid beam-to-column connections. For the pinned connections, the semi-rigid connection model was adapted with substantially reduced spring stiffness values, as proposed in the study. The parameters for the beam-to-column connection element models were selected as follows: for the semi-rigid connections, values of n = 0.98, R_{ki} = 31.635 kN m/rad, and M_u = 142 kNm were used; for the pinned connections, values of $n = 0.9, R_{ki} = 1 \times 10^{-15}$ kNm m/rad, and $M_u = 1 \times 10^{-15}$ kNm were adopted. It is important to note that to simulate the semi-rigid connections, Bui and Kim [15], Bui et al. [14], and the present work used the three-parameter model (3PP), demonstrated in Section 2.1.

The equilibrium paths of the simple frame with concrete-filled rectangular columns and steel beams are detailed in Figure 4. The graph analysis reveals a notable agreement between the numerical results presented by Bui et al. [14] and those obtained in the present analysis. In the case where the connection is considered fully rigid, the initial stiffness and critical load obtained in this work do not perfectly align with the literature results, although the agreement is still satisfactory in the linear and nonlinear phases. When considering the analysis with the semi-rigid connection effect, the convergence is even more expressive, with the curves showing greater proximity.

Furthermore, it is important to highlight that the critical loads from the analysis of the two types of connections are quite close. The difference is only 1.96% for the fully rigid connection and 2.86% for the semi-rigid connection, as presented in Table 1.

Figure 5 shows the equilibrium paths of the simple frame with concrete-filled circular columns and steel beam. The interpretation of the graph reveals a convergence of the results from Bui and Kim [15] and those from this work, especially for the structure with the semi-rigid connection. In the scenario of the fully rigid connection, there is more pronounced convergence in the initial phase, slightly diverging during the initial loss of stiffness.

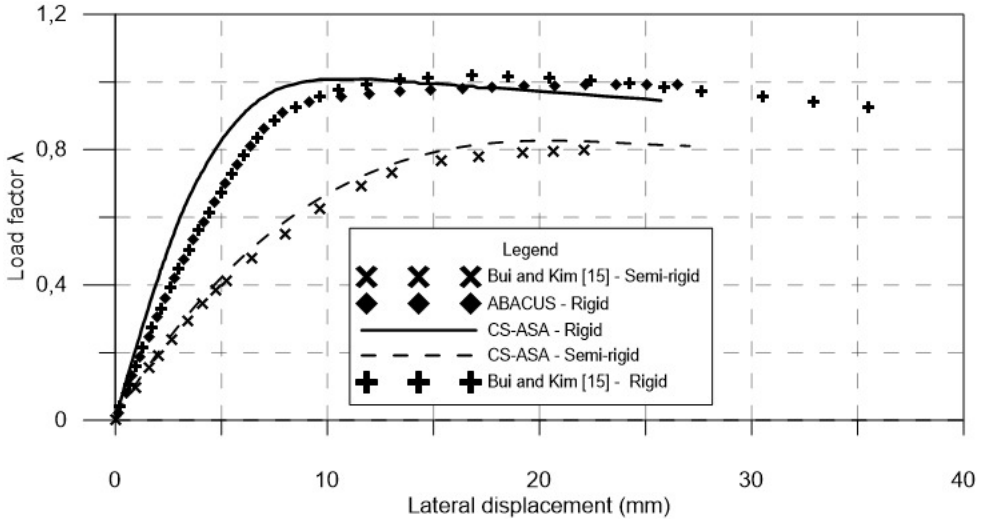

Figure 4. Equilibrium paths of the frame with rectangular column

Table 1. Critical loads of the frame with rectangular column

Connection	CS-ASA	Bui and Kim [15]	Difference
Rigid	0.998	1.018	1.96%
Semi-rigid	0.826	0.803	-2.86%

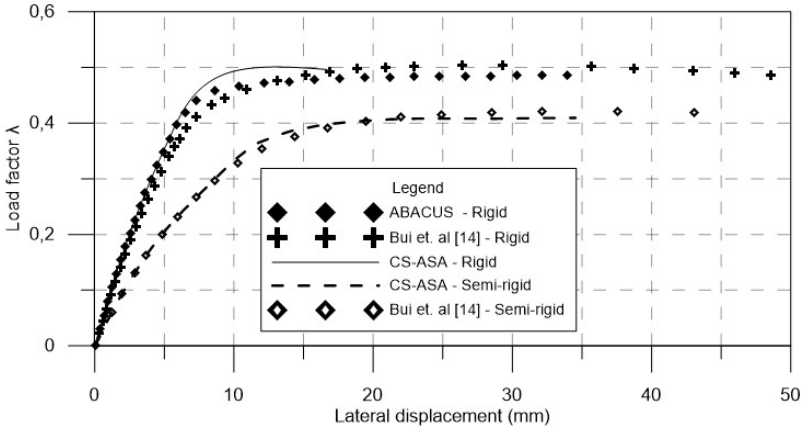

Figure 5. Equilibrium paths of the frame with circular column

Finally, the load limits also show good similarity, with a difference of less than 1% for the fully rigid system and approximately 3% for the structure with the semi-rigid connection, as detailed in Table 2. All these analyses highlight the robustness and coherence of the results generated by the proposed formulation, even in conditions that incorporate the semi-rigid connection between the beam and columns.

Table 2. Critical loads of the frame with circular column

Connection	CS-ASA	Bui et al. [14]	Difference
Rigid	0.500	0.505	-0.99%
Semi-rigid	0.408	0.421	-3.08%

4 Conclusions

The primary scientific contribution of this study is the validation and demonstration of the proposed formulations' effectiveness in accurately capturing the structural behavior of steel-concrete composite frames, incorporating various sources of non-linearities. The simulated examples demonstrated a satisfactory convergence between the results obtained in this study and the numerical and experimental data available in the literature. In both cases, the numerical results were consistent with previous experimental data, validating the accuracy of the proposed formulations.

This consistency underscores the formulation's ability to accurately reproduce the behavior of the analyzed structures. However, it is important to note that while the simplification in evaluating geometric nonlinearity proved valid in all simulations, for very slender structures, it is highly recommended to adopt a co-rotational formulation. This approach ensures more accurate and reliable results, particularly in scenarios involving significant displacements and rotations, with minimal influence of joint semi-rigidity and yield. Additionally, the non-linear joint model (3PP) used in the simulation proved effective, highlighting the robustness of the numerical implementations.

Acknowledgements. The authors acknowledge the financial support of the Brazilian research agencies CNPq and CAPES. They also acknowledge the support of FAPEMIG, PROPPI/UFOP, UFLA, UEMG, Gorceix Foundation and PROPEC/UFOP for their support during the preparation of this work.

Authorship statement. The authors hereby confirm that they are the sole liable persons responsible for the authorship of this work, and that all material that has been herein included as part of the present paper is either the property (and authorship) of the authors, or has the permission of the owners to be included here.

References

[1] I. J. M. Lemes. *Advanced numerical study of steel, concrete and steel-concrete composite structures (in portuguese)*. PhD thesis, Federal University of Ouro Preto, Ouro Preto, MG, Brazil, 2018.
[2] R. B. Caldas. *Análise Numrica de Pilares Mistos Aço-Concreto*. PhD thesis, Universidade Federal de Ouro Preto (UFOP), 2004.
[3] de A. L. A. Oliveira. *Método acoplado integridade e segurança : mais para a avaliação de patrimônios históricos em estruturas de concreto armado*. PhD thesis, Universidade de Brásilia, 2022.
[4] C. Weng and S. Yen. Comparisons of concrete-encased composite column strength provision of aci code and aisc specifications, eng struct 24 (2002). *Elsevier.*, pp. 72, 2002.
[5] A. R. D. Silva. *Sistema computacional para análise avançada estática e dinâmica de estruturas metálicas*. PhD thesis, Programa de Pós Graduação em Engenharia Civil, Universidade Federal de Ouro Preto, Ouro Preto, MG, Brasil, 2009.
[6] W.-F. Chen, Y. Goto, and J. R. Liew. *Stability design of semi-rigid frames*, volume 1. John Wiley & Sons, New York, 1996.
[7] S.-L. Chan and P.-T. Chui. *Non-linear static and cyclic analysis of steel frames with semi-rigid connections*. Elsevier, Oxford, 2000.
[8] M. Fong and S. L. Chan. Advanced analysis of stee-concrete composite beam-columns by refined plastic-hinge method. *Int J Struct Stab Dy*, vol. 12, n. 6, 2012.
[9] J. K. Lee, B. K. Lee, and D. Ahn. Material and geometric nonlinear buckling of simply supported columns. *J Braz Soc Mech Sci Eng*, vol. 45, pp. 40, 2023.
[10] Y. Q. Tang, Z. H. Zhou, and S. L. Chan. Nonlinear beam-column element under consistent deformation. *Int J Struct Stab Dy*, vol. 15, n. 05, pp. 1450068, 2015.
[11] R. D. Ziemian and W. McGuire. Modified tangent modulus approach, a contribution to plastic hinge analysis. *J Struct Eng*, vol. 128, n. 10, pp. 1301–1307, 2002.
[12] Y.-B. Yang and S.-R. Kuo. *Theory and analysis of nonlinear framed structures*. Prentice Hall PTR, 1994.
[13] R. C. Barros, D. Pires, R. A. M. Silveira, Í. J. M. Lemes, and P. A. S. Rocha. Advanced inelastic analysis of steel structures at elevated temperatures by SCM/RPHM coupling. *J Constr Steel Res*, vol. 145, pp. 368–385, 2018.
[14] V.-T. Bui, Q.-V. Vu, V.-H. Truong, , and S.-E. Kim. Fully nonlinear inelastic analysis of rectangular cfst frames with semi-rigid connections. *Steel and Composite Structures*, vol. 38, n. 5, pp. 497–521, 2021.
[15] V.-T. Bui and S.-E. Kim. Nonlinear inelastic analysis of semi-rigid steel frames with circular concrete-filled steel tubular columns. *Journal of Mechanical Sciences*, vol. 196, pp. 1–20, 2021.
[16] ABAQUS. *Standard user's manual*, volume 1, 2 and 3. Hibbitt, USA, 6.8-1 edition, 2008.